



Development and analysis of membranes for osmotic processes

Jader Conceição da Silva*, Cristiano Piacsek Borges

Chemical Engineering Program/COPPE, Federal University of Rio de Janeiro, Cidade Universitária, Rio de Janeiro, 21945-970 RJ, Brazil, Tel. +55 21 3938-8349/+55 21 3938-8304; Fax: +55 21 3938-8300, emails: jader@peq.coppe.ufrj.br (J.C. da Silva), cristiano@peq.coppe.ufrj.br (C.P. Borges)

Received 7 October 2015; Accepted 25 December 2016

ABSTRACT

Osmosis is a phenomenon widely studied in several knowledge areas like biology and chemistry. Many researches focus it in food production, desalination, water treatment, drinking water production and citric juices aroma concentration. According to the necessity of electric power supply, this phenomenon can use to convert free energy of a mixture in electric energy by the osmotic pressure gradient across a selective membrane. Osmosis is a process operated on the principle of solvent (water) transport across a selectivity membrane from a low salinity feed solution into a high salinity solution, named draw solution. In membrane science, to achieve the required membrane energy density, it is necessary to control the transport properties of the membrane. In this study, anisotropic membranes with a cellulose acetate selective layer were prepared by phase inversion simultaneously casting two polymer solutions, one for the selective layer and another for the porous support. In addition, reverse osmosis and nanofiltration commercial membranes were also evaluated and their results compared with membranes prepared by phase inversion. Synthesized membranes showed high osmotic flux ($\sim 6.5 \text{ L/h m}^2$) by using a draw solution with sodium chloride (0.5 M) and deionized water as feed solution and the greater membrane coefficient permeability was $2.46 \text{ L/h m}^2 \text{ bar}$.

Keywords: Forward osmosis; Pressure retarded osmosis; Energy generation; Membrane

1. Introduction

World economic and social growth are directly associated to the global energy availability and the current global energy demand far exceeds our capacity of production. The oil importance's is recognized worldwide, but energy based in fossil fuels has been related to emission of greenhouse gases and air pollutants increases [1]. In addition, shortages matters, oscillation prices and environmental issues have motivated the investment in development of alternative energy sources [2,3].

A large amount of energy is irreversibly dissipated in estuaries. Each second thousands of cubic meters of river water with low salinity flow freely into the sea with high salinity. This natural river discharge can be used to generate sustainable energy. The seawater or ocean water evaporates

and it is transported through clouds and subsequently precipitates like freshwater. This freshwater is a diluted salt solution, which is transported through rivers toward the sea and/or oceans to close the natural cycle [4,5]. The discharge of river water into the sea dissipates chemical energy, which could be transformed into electrical energy by osmotic phenomenon, in a process known as pressure retarded osmosis (PRO) [5]. It is estimated that the global energy production potential of PRO is approximately 2,000 TWh per year, while the estimated global energy production from all renewable sources is nearly 10,000 TWh per year [6].

Currently, the problem is to convert this free energy of mixing to electric energy by economic means. To achieve a feasible PRO process, the power generated per unit membrane area should be about 5 W/m^2 [3,7]. Pattle [8] reported for the first time about electric power generation from salinity gradient by the osmotic phenomenon. Since this publication until the mid-1970s very few publications can be noticed

* Corresponding author.

related to the theme. However, the oil crisis in 1973 brought back the interest in power generation process by osmotic phenomena, well marked by a number of significant publications. Loeb was the first author to analyze the technical feasibility and to report an economical evaluation of PRO [9,10]. The major challenge was to adapt existing reverse osmosis (RO) membrane to the PRO process.

RO membranes are asymmetric, exhibiting a dense skin upon a porous support designed to withstand high hydraulic pressures. This characteristic configures high resistance to mass transport through the membrane, generating low osmotic fluxes and intense reverse salt flux, which contributes to driven force drop and lower membrane power density (W/m^2) [10]. To improve PRO it is necessary to understand the relationship between membrane morphology and mass transfer parameters. To obtain more insight about the influence of membrane morphology and its transport properties on the forward osmosis (FO) phenomenon, this paper evaluated commercial membranes and membranes that were synthesized by phase inversion technique.

2. Literature review

2.1. Osmotic phenomenon

Osmosis is the transport of solvent through a selective membrane from a solution with lower salt concentration (i.e., lower osmotic pressure) to a solution of high salt concentration until chemical potential equilibrium [4,11]. The selective membrane allows water passage and retains the solute. Currently, the scientific literature highlights basically the following osmotic processes: RO, PRO and FO. In RO, the hydraulic pressure difference through the membrane is greater than the osmotic pressure difference, while in FO the hydraulic pressure difference is zero. PRO is an intermediate process between FO and RO [12,13], where solvent and solute are transported in the opposite directions, so that water flux is against the hydraulic pressure difference, allowing energy production [14]. Fig. 1 illustrates the directions of water and solute fluxes in FO, PRO and RO.

The water transport (osmotic flux) and the membrane power density are described by Eqs. (1) and (2):

$$J_w = A(\Delta\pi - \Delta P) \tag{1}$$

$$W = J_w \Delta P = A(\Delta\pi - \Delta P)\Delta P \tag{2}$$

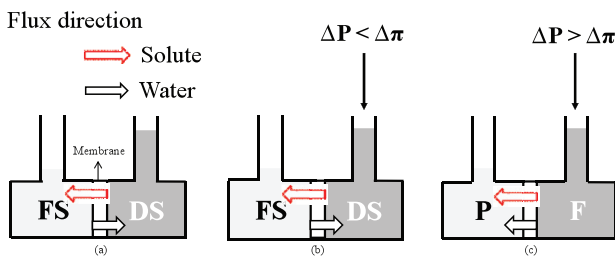


Fig. 1. Schematic representation of membrane and flux directions in (a) FO, (b) PRO and (c) RO.

where J_w is the water flux, A is the water permeability coefficient of the membrane, ΔP is the hydraulic pressure difference, $\Delta\pi$ is the osmotic pressure difference and W is the membrane power density.

The membrane power density has a parabolic profile as a function of ΔP , and the maximum value is achieved when $\Delta P = \Delta\pi/2$. Replacing ΔP into Eq. (2), the maximum membrane power density can be easily determined, Eq. (3). Fig. 2 shows the osmotic flux and the membrane power density as a function of the hydraulic pressure difference.

$$W = A \frac{(\Delta\pi)^2}{4} \tag{3}$$

In Fig. 2, null hydraulic pressure difference represents the FO process conditions. PRO occurs from this condition till $\Delta P < \Delta\pi$, while RO region is characterized by $\Delta P > \Delta\pi$. There is no osmotic flux when $\Delta P = \Delta\pi$, and it is considered as a point of transition between PRO and RO.

In the gray curves the ideal condition is shown. In this situation, it is implicit that there is a total rejection to the solute ($R = 1$) and the feed solution (FS) concentration is zero. Only the solvent is permeated across the membrane, and the concentration polarization (CP) and membrane resistance (K) are neglected. The FS and draw solution (DS) concentrations remain unchanged during the entire process. These curve profiles are plotted by Eq. (1) (ideal flux) and Eq. (2). The blue curves show the real condition. In all membrane separation processes CP is present and it must be minimized. In the PRO operations, there are water and reverse salt flux concurrent permeations. The solute diffusion from concentrated to diluted solution causes the simultaneous DS concentration reduction and FS concentration increase, resulting in the effective osmotic pressure difference through the membrane.

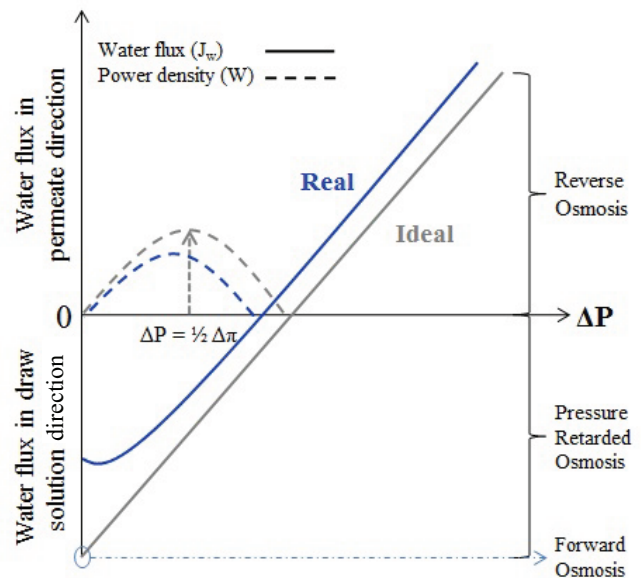


Fig. 2. Osmotic flux and membrane power density in FO, PRO and RO as a function of the hydraulic pressure difference. Adapted from Lee et al. [4].

The real-flux profile can be represented in graphic by plotted Eq. (11) and corresponding density energy generated can be calculated by the product with the hydraulic pressure difference.

In PRO, the salt diffusion from high salinity solution (DS) to low salinity solution (FS) still is the main limitation to be overcome, since it leads to reduction in the driven force for the process. The salt permeability coefficient can be estimated by RO experiments by Eqs. (4) and (5):

$$B = \frac{A(1-R)(\Delta P - \Delta\pi)}{R} \quad (4)$$

$$R = 1 - \frac{C_p}{C_c} \quad (5)$$

where B represents salt permeability coefficient, R is the salt rejection, C_p and C_c are the solute concentration in the permeate and concentrate streams, respectively.

FO and PRO membranes are usually asymmetric, consisting of a thin dense layer upon a microporous support and another limiting factor of these processes is the CP phenomenon, which is related to the increase or decrease of the solute concentration near to the interface between the membrane and the solutions [13]. When CP occurs outside of the dense layer this phenomenon is named as external polarization concentration (ECP). In the other hand, when it takes place within the porous support it is called internal polarization concentration (ICP), as illustrated in Fig. 3.

By convention, the water flux headed to the DS is considered negative and it leads to dilution of the solution near the membrane surface ($\pi_{D,m} < \pi_{D,b}$). Increasing the flow velocity can effectively control ECP, however, ICP is more difficult to handle. The film theory can be applied to estimate the external CP modulus, as described in Eqs. (6)–(8):

$$\frac{\pi_{D,m}}{\pi_{D,b}} = \exp\left(-\frac{J_w}{k}\right) \quad (6)$$

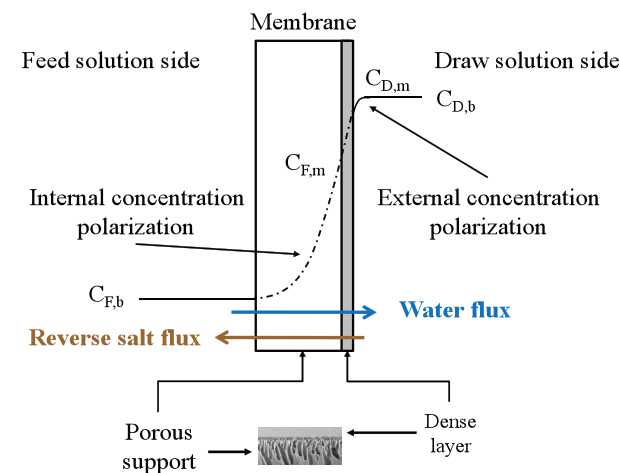


Fig. 3. Illustration of asymmetric membrane, internal and external concentration polarization and flux directions in FO. Adapted from Loeb et al. [15].

$$k = \frac{ShD}{d_H} \quad (7)$$

$$Sh = a \cdot Re^b Sc^c \quad (Re < 1,000) \quad (8)$$

where $\pi_{D,m}$ and $\pi_{D,b}$ are osmotic pressure near the membrane surface and in bulk DS, respectively, k is the mass transport coefficient, D is the solute diffusion coefficient, d_H is the hydraulic diameter, Sh , Sc and Re are the Sherwood, Schmidt and Reynolds numbers, respectively, a , b and c are constant parameters.

In ICP, the solute molecules are within the porous substrate, where it is very difficult to improve the mass transfer conditions, and its control is considered as a key element in FO and PRO processes. The film theory can also describe the ICP and, according to Lee et al. [4], the osmotic flux can be expressed by Eqs. (9) and (10):

$$J_w = A \left(\pi_{D,m} \frac{1 - \frac{C_{F,b}}{C_{D,m}} \exp(J_w K)}{1 + \frac{B}{J_w} [\exp(J_w K) - 1]} - \Delta P \right) \quad (9)$$

$$K = \frac{t\tau}{D\varepsilon} \quad (10)$$

where $C_{F,b}$ is the bulk solute concentration in FS, $C_{D,m}$ is solution concentration at the membrane surface in DS, K is the solute diffusion resistivity within the porous support, t , τ , and ε are the thickness, tortuosity, and porosity of the support, respectively.

To estimate concentration at membrane surface Loeb et al. [15] proposed the approximation ($\pi_{F,b}/\pi_{D,m}$) = ($C_{F,b}/C_{D,m}$). Substituting $\pi_{D,m}$ from Eq. (6) in Eq. (9) the osmotic flux in PRO can be expressed by Eq. (11).

$$J_w = A \left(\pi_{D,b} \exp\left(-\frac{J_w}{k}\right) \frac{1 - \frac{\pi_{F,b}}{\pi_{D,m}} \exp(J_w K) \exp\left(\frac{J_w}{k}\right)}{1 + \frac{B}{J_w} [\exp(J_w K) - 1]} - \Delta P \right) \quad (11)$$

In Eq. (11), J_w is function of the solution properties, membrane characteristics and applied hydraulic pressure difference. The osmotic flux in FO can be calculated when $\Delta P = 0$.

The solute diffusion resistivity within the porous can be calculated experimentally from FO ($\Delta P = 0$) by using deionized water ($C_{F,b} = 0$) as the FS. The membrane power density is calculated by the product between the osmotic flux and hydraulic pressure difference.

2.2. Membranes for osmotic power generation

In recent years, the development of PRO membranes has attracted increasing interest in renewable osmotic power. The academy has made continuous efforts to fabricate membranes with higher water permeability and solute rejection. In the experimental osmotic processes for power generation,

the salt and water are transported simultaneously, in opposite directions: water from FS to DS and salt (reverse salt flux) from DS to FS. It is necessary to make a balance between water flux and reverse salt flux for the transfer of molecules between each side, since it isn't possible to block the salt passage. A high value for B parameter means that there will be a fast solute passage from DS to FS. It will increase the FS concentration and it will decrease both, osmotic pressure difference ($\Delta\pi$) and the energy generated. This aspect is noted by Eq. (9) analysis. However, if the mass transfer competition between reverse salt flux and water flux is not controlled it can contribute to the low power generated by the membrane area which is the main limitation in PRO process. In literature, the mass transfer competition is related by the ratio of reverse salt flux to water flux [16,17]. Phillip et al. [18], Xie et al. [19] and Yong et al. [20] classified this relationship as reverse salt flux selectivity that is defined as the ratio of water osmotic flux to reverse salt flux. To overcome these obstacles, different authors are concentrating efforts to improve membrane development: selectivity and permeability. Zhang et al. [21] fabricated TFC flat-sheet membranes on polyacrylonitrile supports with ethanol post-treatment and the theoretical results showed that after the post-treatment the water flux increased from 20 to 40 L/h \times m² and the power density was about 6 W/m². In attempt to obtain suitable membranes some authors focus their studies in cylindrical geometry and different techniques in membrane synthesis. By the interfacial polymerization, Han et al. [22] synthesized hollow fiber (HF) membranes with polyamide (PA) selective layer supported by Matrimid material. The authors reported that in PRO mode operation working at 16 bar a power density of 14 W/m² was obtained using 1.0 mol/L NaCl as DS and deionized water as FS. Through the same technique Wan and Chung [23] manufactured thin-film composite membrane, composed by PA onto polyethersulfone (PES) support. In order to minimize the environmental impact, this study used the discharging of the concentrate brine of RO process as DS. Researchers have reported that, when the following conditions, deionized water as FS and 20 bar pressure difference were fixed and 1.0 M sodium chloride and seawater brine were used as DSs, the maximum power densities were obtained, respectively, 27.0 and 21.1 W/m². These results have been calculated by simulation model. Li and Chung al. [24] realized a detailed study of membrane synthesis directed to geometry spinneret and its dimension to control phase inversion process during spinning. Using a copolyimide as a selective layer the authors demonstrated that maximum power density 12 W/m² was obtained when 21 bar pressure and 1.0 M NaCl were used. According to Gai et al. [25], there has been a development of a systematic study about HF membranes deformation and its influence in osmotic power generation. The HF membranes were synthesized by PES substrates and PA selective layer. The main variables monitored were water flux, reverse salt flux and power density. The authors have recognized that it is still difficult to connect selectivity to osmotic flux and power density. On the other hand, even with this limitation, the researchers showed that the HF mechanical stabilization can increase 60% more to the power density. In this paper, researchers evaluated reverse salt flux in FO mode ($\Delta P = 0$) for five thin-film composite membranes and they obtained

a range from 13.14 to 16.79 g/m² h (0.0060–0.0077 L/m² h). It was also verified that between 0 and 5 bar there were no observed significant differences in reverse salt flux. Cheng et al. [16] synthesized thin-film HF membranes composed by PES supports and a PA selective layer to generate energy. In this study, non-solvent polyethylene glycol was used into the spinning dopes aiming to improve pore interconnectivity. Their results showed that thin-film membranes presented low salt permeability between 0.022 and 0.042 L/m² h. The literature review had demonstrated that there are no specific rules or tendencies to compare PRO tests and can be seen by the different hydraulic pressure shown in the papers.

3. Materials and methods

In this study only FO tests are performed.

3.1. Commercial membranes and draw solutions

The commercial membranes tested were PA thin-film composite BW30 and NF90 (DOW FILMTEC™), and cellulose triacetate (CTA) (Hydration Technology Innovations, Albany, OR). The BW30 membrane was used with and without non-woven support. Sodium chloride (0.5 M) and deionized water were used as DS and FS, respectively. Table 1 shows DS properties obtained by extrapolation of data from Achilli et al. [12].

3.2. Flat-sheet membranes by phase inversion

Flat-sheet membranes were prepared by phase inversion using immersion precipitation technique. The membranes were obtained by simultaneous casting of two polymers solutions. Cellulose acetate (CA) (Sigma-Aldrich, Brazil, SP) was used as a selective layer and polyetherimide (PEI) (Ultem resin, GE) to form the porous support. *N*-Methyl-2-pyrrolidone (NMP) (Sigma-Aldrich) was used as solvent to both polymers; formamide (FM) and polyvinylpyrrolidone (PVP) (K90, Fluka) were used as additive to CA and PEI solutions, respectively. After casting, solutions were immediately immersed into distilled water as the precipitation bath, and after precipitation, the membranes were kept immersed in water at 60°C overnight, for residual solvent extraction. Membrane casting system is shown in Fig. 4.

Initially, the polymeric solutions were prepared by mechanical stir. After, the solution was poured on the glass plate and immediately casted with a knife about 200 μ m of thickness. In this work, the simultaneous casting was accomplished by two castings within a small difference of time. First, the porous support polymeric solution was spread on a glass plate and after, in the same plate, skin polymeric solution was spread on porous support polymeric, which was

Table 1
Properties of NaCl (0.50 M) aqueous solution

π (bar)	23.20
μ (mPa s)	0.929
ρ (g/L)	1.017
D (10 ⁻⁹ m ² /s)	1.481

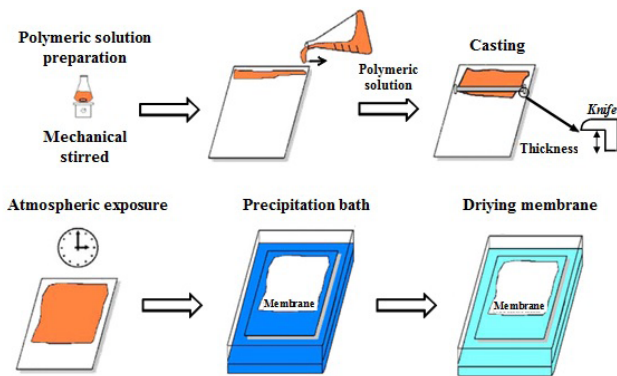


Fig. 4. Casting polymer solutions representation.

Table 2
Solutions compositions (wt%) used to prepare membranes by phase inversion

Selective layer (SL) CA/FM/NMP	Porous support (PS) PEI/PVP/NMP	Membrane
SL1 12/0/88	PS1 15/10/75	SL1–PS1
SL2 20/0/80	15/10/75	SL2–PS1
SL3 26.7/23.3/50	15/10/75	SL3–PS1
SL2 20/0/80	PS2 15/0/85	SL2–PS2

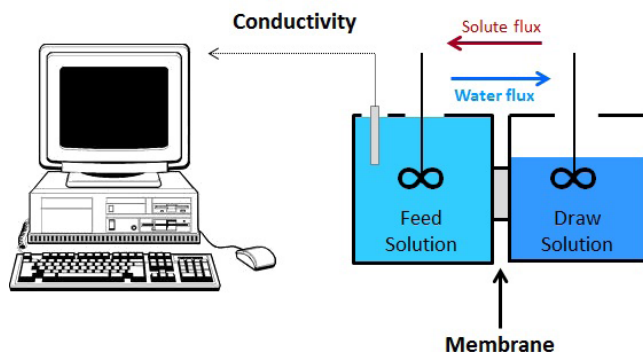


Fig. 5. FO permeation apparatus with two stirred compartments.

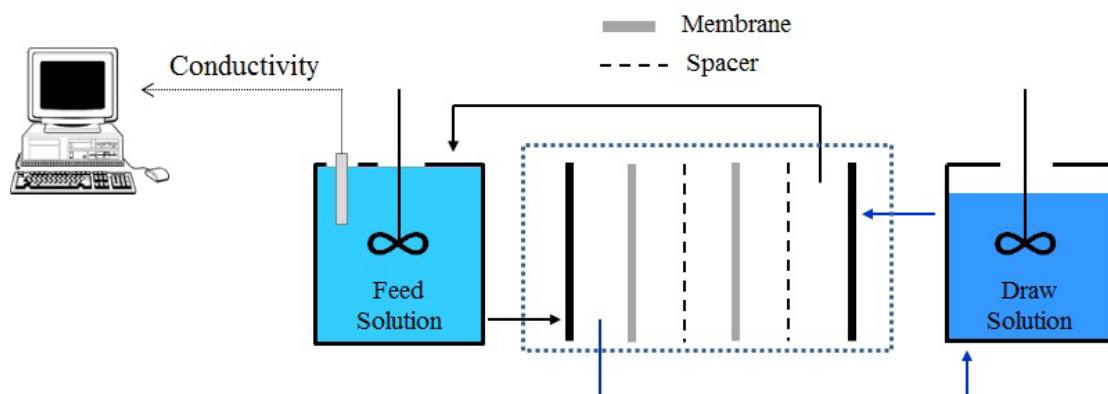


Fig. 6. FO permeation apparatus with plate-and-frame membrane module.

casted previously. The membrane obtained was exposed at room temperature in a time range settled. Sequentially, the glass plate and polymeric solutions casted were immersed into a precipitation bath. The simultaneous casting advantage is to combine different polymers characteristics in membrane like cellulosic materials that are hydrophilic and PEI which is hydrophobic material.

Table 2 presents the solutions compositions used for membrane preparation. These conditions were chosen to obtain different membrane morphologies [26], allowing investigation of its influence on the membrane permeability, osmotic flux and reverse salt flux. For all prepared membranes, the transport properties were determined and its morphology analyzed by a scanning electron microscope (SEM).

The additives FM and PVP were doped, respectively, in polymer solutions to form asymmetric membranes and hydrophilic support porous.

3.3. Permeation apparatus

The membranes were tested in FO using two permeation apparatus, one with two compartments where the solutions were constantly stirred (~350 rpm) and circa of 25 cm² of permeation area (Fig. 5). In the other permeation system, the DS and FS were circulated through a plate-and-frame cell with about 900 cm² of permeation area (Fig. 6).

The basic difference between the systems is the hydrodynamics flow and available membrane area. In the first system (Fig. 5), the solutions contact the membrane and both are stirred. In this situation, the FS volume was about 2.5 times higher than DS. Thus, the reverse salt flux was monitored by the conductivity meter cell submerged in FS, and the osmotic flux was measured through relationships between membrane area (25 cm²) and volume change in DS at time range. At the second apparatus was a plate-and-frame membrane module. In this system, the solutions were pumped from the two tanks to module. Both DS and FS were not directly stirred in bulks solutions. The total membrane area permeation was about 900 cm². In this case, the transport parameters were tracking similarly like the first one. The main objective of the study of these systems was to investigate the transfer of components across the membrane in distinct flow forms (pumping or stirring) in a greater scale of membrane area and their influences on the osmotic flux and reverse salt flux. In a large

scale, the reverse salt flux is still the principal limitation for FO permeation. Therefore, it is important to check the differences between membrane area and hydrodynamics and their influences on transport parameters, like in reverse salt flux and osmotic flux.

In this study, membranes were analyzed only at FO tests and the determination of membrane characteristics like membrane permeability and salt rejection were obtained through RO tests as proposed by Achilli et al. [12].

4. Results and discussion

4.1. Membranes by phase inversion

4.1.1. Membrane morphology

Fig. 7 shows the photomicrographs of the cross-sections, bottom and top surfaces of membranes prepared by phase inversion. The conditions are described in Table 2. In the photomicrographs of Fig. 7 a very good adhesion or even

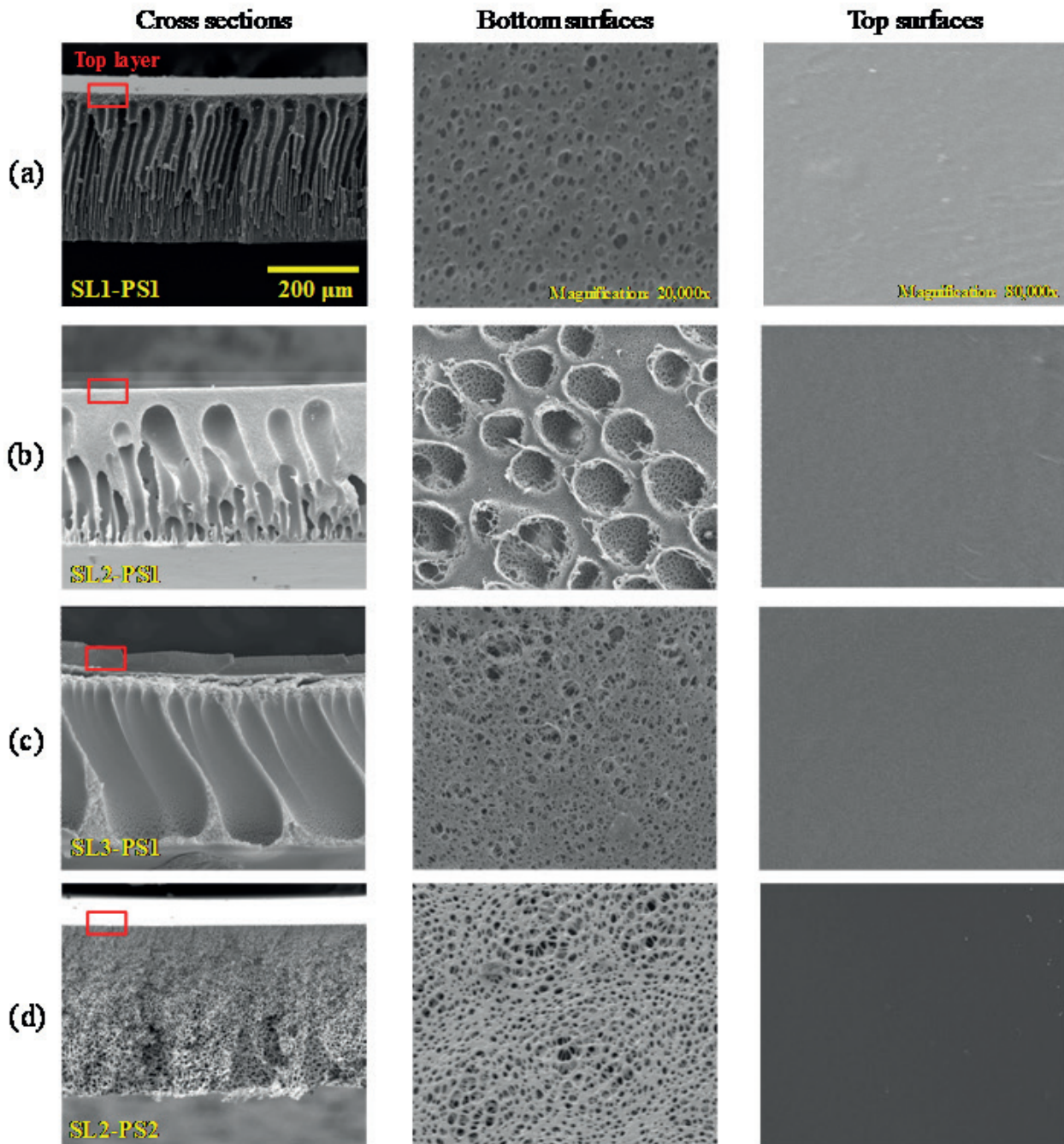


Fig. 7. Photomicrographs of the cross-sections, bottom (magnification 20,000×) and top (magnification 80,000×) of the membranes prepared by phase inversion.

total interpenetration of CA and PEI solutions can be noticed. Only for SL3-PS1 membrane is it possible to observe a clear interface between the two polymer phases. This membrane was prepared by using FM as additive to CA solution, which can accelerate its precipitation avoiding a complete interpenetration with PEI solution. Large macrovoids in PEI solution are also consequence of CA solution precipitation, which creates an extra barrier to mass exchange with the precipitation bath.

Macrovoids were almost suppressed when no additives were added to CA and PEI solution, which could be related to a fast mixing of the solutions approaching them to the liquid-liquid separation region. Macrovoids in membranes SL1-PS1 and SL2-PS1 differ in number and size, which also could be related to the increase in the interfacial resistance to mass transfer promoted by higher CA concentration. Furthermore, it should be considered that NMP is a good solvent for CA and PEI and, according to Yip et al. [2], good solvents cause the non-solvent diffusion front to move faster than the vitrification front, sustaining the driving force to macrovoids formation.

4.1.2. Water permeability and saline rejection

For all synthesized membranes, Fig. 8 shows the water permeate flux as a function of hydraulic pressure difference through the membrane and Table 3 presents the water permeability and NaCl rejection of each membranes.

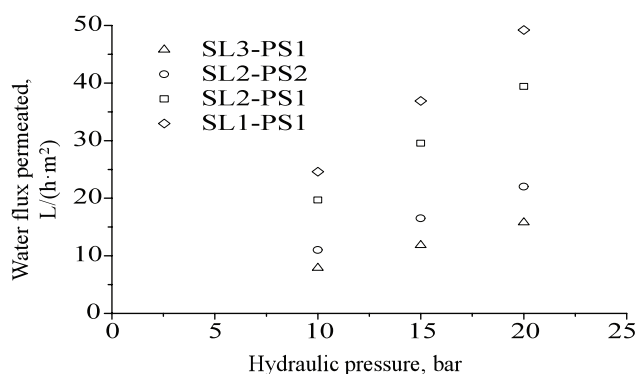


Fig. 8. Water flux permeated profile in RO mode.

Table 3

Water permeability (A) and saline rejection (R%) of the membranes prepared by phase inversion

	Water permeability, L/(h m ² bar)	Rejection (%)
SL1-PS1	2.46	33.0
SL2-PS1	1.97	65.4
SL3-PS1	0.79	75.5
SL2-PS2	1.10	44.5

Note: Permeability and rejection values were calculated from RO tests. $\Delta P = 15$ bar and feed with 2 g/L NaCl.

It is very clearly that the increase in CA concentration in the polymeric solution and PVP as additive in the porous support has influence on the water permeability. Higher CA concentration in SL2-PS1 and SL3-PS1 membranes reduces the water permeability and increases the saline rejection, as a consequence of a denser top layer. The membrane SL2-PS2 was prepared without PVP in the support layer solution, with favored mixing of CA and PEI mixture, promoting nucleation of a polymer lean phase and higher porosity and, consequently, good water permeability characteristics. However, there is a water permeability difference between SL1-PS1 and SL2-PS2 membranes. This discrepancy is understood as the chemical interaction between water and PVP and PEI polymers during permeability tests. According to Hansen [27], solubility parameters, the nitrogen and oxygen groups make the PVP water solubility higher when it is compared with PEI, which these groups are further way from each other. Furthermore, PEI has carbonic rings that provide hydrophobicity to the polymer. Fig. 9 shows the polymers monomeric units.

Conversely, the lowest saline rejection and the highest water permeability were obtained with lowest CA concentration. The PVP polymer is more hydrophilic than the other ones due the oxygen and nitrogen group contributions. This fact, makes the porous support wetted decreasing mass transport resistance in this membrane region. The PVP presence in polymeric solution increases the membrane hydrophilicity and that can be seen in Table 3 comparing the SL2-PS2 and SL2-PS1.

4.1.3. Diffusion resistivity (K) and salt permeability (B)

The diffusion resistivity is related to ICP intensity and the salt permeability may reduce the water flux in the osmotic process. Both contribute to driving force decline and have to be minimized. The main mechanisms and parameters that govern internal CP are molecular size, membrane selectivity, water flux and the porous support structure. According to RO theory, the membrane that has a high selectivity increases a solute concentration near the membrane surface and it will increase the osmotic pressure and resulting in the reduction

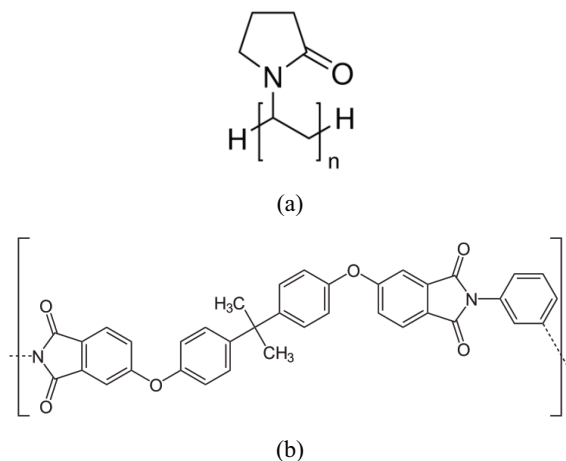


Fig. 9. Monomeric units of (a) PVP and (b) PEI.

of the osmotic/water flux if the hydraulic pressure is not raised. This behavior can be noted by the ΔP and $\Delta\pi$ shift position in Eq. (1). Therefore, PRO high rejections can support the solute passage from DS to FS and it consequently will reduce both osmotic pressure difference and the maximum power density as shown in Eq. (3). Moreover depending on membrane structure, solute can remain into porous support and build physical barrier, and it contributes to flux reduction.

On the other hand, the balance and control between osmotic flux and selectivity can produce acceptable levels for these parameters. Therefore, the 75.5% is a value rejection that can minimize the internal CP. The diffusion resistivity and the salt permeability are obtained experimentally by FO and RO tests, respectively. Fig. 10 shows the comparison of diffusion resistivity for all membranes prepared by phase inversion and Table 4 presents the salt permeability of these membranes.

As expected the lowest salt permeability was obtained by the membrane prepared with the highest CA concentration (SL3-PS1), but it was associated with the highest diffusion resistivity. However, as observed by SEM, this membrane exhibits large macrovoids that should facilitate the solute diffusion. Therefore, it can be concluded that the top layer resistance is the limiting step to the salt transport, including the diffusion to the DS. The diffusion resistivity and the salt permeability for the other membranes follow the expected tendency like demonstrated by the water permeability and saline rejection values.

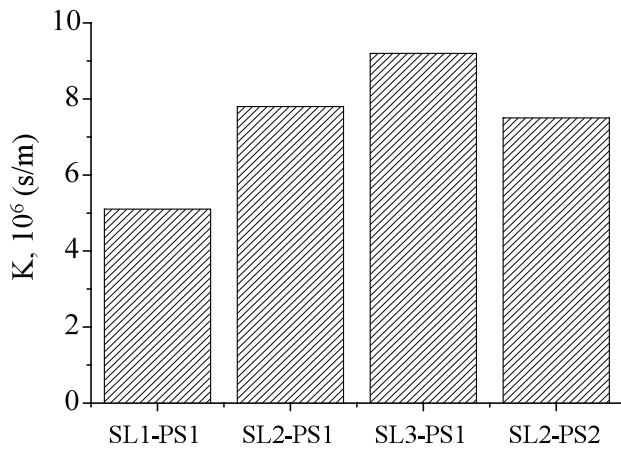


Fig. 10. Diffusion resistivity of the membranes prepared by phase inversion. Permeation apparatus: stirred compartments.

Table 4
Salt permeability of the membranes prepared by phase inversion

	B (L/m ² h)
SL1-PS1	0.02621
SL2-PS1	0.00306
SL3-PS1	0.00133
SL2-PS2	0.01288

4.2. Osmotic flux and reverse salt flux

The osmotic flux and reverse salt flux were measured in commercial and synthesized membranes by using a plate-and-frame module, as portrayed in Fig. 11. For the sake of comparison, the non-woven fabric of BW30 membrane was carefully removed before permeation tests and this membrane was named as BW30 snw.

All the membranes are selective to water permeation. Membranes prepared by phase inversion show higher osmotic flux than RO and NF commercial membranes, and comparable to the osmotic flux of CTA membrane, which is commercially available for FO. The lowest reverse salt flux was observed in the BW30 membrane, which increases after the non-woven removal, similarly as detected in the osmotic flux. It is an indication that this support offers an extra transport resistance for the FO process.

The reverse salt flux increases for NF and CTA commercial membranes, probably due to a less dense selective layer of these membranes. All the synthesized membranes exhibited had lower reverse salt flux than the BW30 snw membrane, corresponding about one-third of the reverse salt flux of CTA membrane.

It can be seen that experimental results are consistent to morphological characteristics of the membranes, i.e., lower

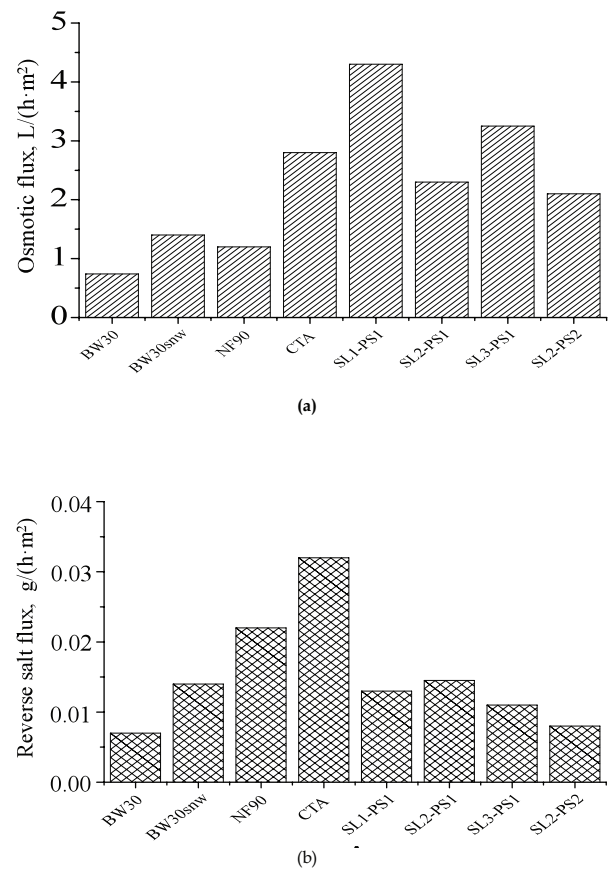


Fig. 11. Osmotic (a) and reverse salt (b) fluxes for synthesized membranes and commercial membranes. Permeation apparatus: plate-and-frame.

porosity, higher tortuosity and thickness imply a greater resistance to the passage of solute. The results are also consistent with the intensity of the solute flux from DS to FS, which augments the osmotic pressure of the diluted solution ($\pi_{F,b}$) and reduces the driving force of water permeation through the membrane.

5. Conclusions

The osmotic flow and the reverse salt fluxes are very dependent on the porous support resistance, since the internal CP is one of the main limiting factors in FO and PRO. Low solute resistivity is observed with membrane morphology with a thin skin layer above finger-like pores, e.g., SL1–PS1 membrane. On the other hand, membranes with sponge-like porous support, e.g., SL2–PS2, tend to exhibit high solute resistivity, mainly because of solute back diffusion. Commercial membranes for RO or NF cannot be used in FO or PRO because their support resistance leads to low reverse salt flux and water permeate flux. The non-woven support of the commercial membranes also exerts resistance to the solute transport and should be avoided.

Acknowledgments

The authors thank the CNPq – The Brazilian Council of Research and Development for the scholarship, Tractebel Energy for their support during the research and Hydration Technology Inc. for providing membranes.

Symbols

J	–	Water flux, L/h m ²
A	–	Water permeability coefficient, L/h m ² bar
W	–	Power density, W/m ²
B	–	Salt permeability, m/s
R	–	Rejection
C	–	Concentration, mol/L
k	–	Mass transport coefficient, m/s
K	–	Solute diffusion resistivity, s/m
D	–	Diffusion coefficient, m ² /s
t	–	Thickness, m
d	–	Diameter, m
Sh	–	Sherwood number
Sc	–	Schmidt number
Re	–	Reynolds number
a, b and c	–	Constant parameters
HF	–	Hollow fiber
PES	–	Polyethersulfone
PA	–	Polyamide
CTA	–	Cellulose triacetate
CA	–	Cellulose acetate
FM	–	Formamide
NMP	–	<i>N</i> -Methyl-2-pyrrolidone
PEI	–	Polyetherimide
PVP	–	Polyvinylpyrrolidone
SL	–	Selective layer
PS	–	Porous support
FS	–	Feed solution
DS	–	Draw solution
P	–	Permeated
F	–	Feed

Greek

τ	–	Tortuosity
ε	–	Porosity
π	–	Osmotic pressure, bar
ΔP	–	Hydraulic pressure difference, bar
$\Delta\pi$	–	Osmotic pressure difference, bar

Subscripts

W	–	Water
P	–	Permeated
C	–	Concentrated
F, b	–	Bulk solute in feed solution
D, m	–	Membrane surface in draw solution
H	–	Hydraulic

References

- [1] L. Panyor, Renewable energy from dilution of salt water with fresh water: pressure retarded osmosis, *Desalination*, 199 (2006) 408–410.
- [2] N.Y. Yip, A. Tiraferri, W.A. Phillip, J.D. Schiffman, L.A. Hoover, Y.C. Kim, M. Elimelech, Thin-film composite pressure retarded osmosis membranes for sustainable power generation from salinity gradients, *Environ. Sci. Technol.*, 45 (2001) 4360–4369.
- [3] X. Wang, Z. Huang, L. Li, S. Huang, E.H. Yu, K. Scott, Energy generation from osmotic pressure difference between the low and high salinity water by pressure retarded osmosis, *J. Technol. Innov. Renew. Energy*, 1 (2012) 122–136.
- [4] K.L. Lee, R.W. Baker, H.K. Lonsdale, Membranes for power generation by pressure-retarded osmosis, *J. Membr. Sci.*, 8 (1981) 141–171.
- [5] P.E. Długolecki, Mass Transport in for Sustainable Energy Generation, PhD Thesis, University of Twente, The Netherlands, 2009.
- [6] R.J. Aaberg, Osmotic power: a new and powerful renewable energy source?, *Refocus*, 4 (2003) 48–50.
- [7] T. Thorsen, T. Holt, The potential for power production from salinity gradients by pressure retarded osmosis, *J. Membr. Sci.*, 335 (2009) 103–110.
- [8] R.E. Pattle, Production of electric power by mixing fresh and salt water in the hydroelectric pile, *Nature*, 174 (1954) 660.
- [9] S. Loeb, Production of energy from concentrated brines by pressure-retarded osmosis: I. Preliminary technical and economic correlations, *J. Membr. Sci.*, 1 (1976) 49–63.
- [10] S. Loeb, F. van Hesses, D. Shahaf, Production of energy from concentrated brines by pressure-retarded osmosis: II. Experimental results and projected energy costs, *J. Membr. Sci.*, 1 (1976) 249–269.
- [11] R. Patel, W.S. Chi, S.H. Ahn, C.H. Park, H. Lee, J.H. Kim, Synthesis of poly(vinyl chloride)-*g*-poly(3-sulfopropyl methacrylate) graft copolymers and their use in pressure retarded osmosis (PRO) membranes, *Chem. Eng. J.*, 247 (2014) 1–8.
- [12] A. Achilli, T.Y. Cath, A.E. Childress, Power generation with pressure retarded osmosis: an experimental and theoretical investigation, *J. Membr. Sci.*, 343 (2009) 42–52.
- [13] R.W. Baker, *Membrane Technology and Applications*, 2nd ed., John Wiley & Sons, Ltd., West Sussex, UK, 2004.
- [14] F. Helfer, C. Lemckert, Y.G. Anissimov, Osmotic power with pressure retarded osmosis: theory, performance and trends – a review, *J. Membr. Sci.*, 453 (2014) 337–358.
- [15] S. Loeb, L. Titelman, E. Korngold, J. Freiman, Effect of porous support fabric on osmosis through a Loeb-Sourirajan type asymmetric membrane, *J. Membr. Sci.*, 129 (1997) 243–249.
- [16] Z.L. Cheng, X. Li, Y.D. Liu, T.-S. Chung, Robust outer-selective thin-film composite polyethersulfone hollow fiber membranes with low reverse salt flux for renewable salinity-gradient energy generation, *J. Membr. Sci.*, 506 (2016) 119–129.

- [17] N.T. Hancock, T.Y. Cath, Solute coupled diffusion in membrane processes, *Environ. Sci. Technol.*, 43 (2009) 6769–6775.
- [18] W.A. Phillip, J.S. Yong, M. Elimelech, Reverse draw solute permeation in forward osmosis: modeling and experiments, *Environ. Sci. Technol.*, 44 (2010) 5170–5176.
- [19] M. Xie, W.E. Price, L.D. Nghiem, M. Elimelech, Effects of feed and draw solution temperature and transmembrane temperature difference on the rejection of trace organic contaminants by forward osmosis, *J. Membr. Sci.*, 438 (2013) 57–64.
- [20] J.S. Yong, W.A. Phillip, M. Elimelech, Coupled reverse draw solute permeation and water flux in forward osmosis with neutral draw solutes, *J. Membr. Sci.*, 392–393 (2012) 9–17.
- [21] S. Zhang, P. Sukitpaneevit, T.-S. Chung, Design of robust hollow fiber membranes with high power density for osmotic energy production, *Chem. Eng. J.*, 241 (2014) 457–465.
- [22] G. Han, P. Wang, T.-S. Chung, Highly robust thin-film composite pressure retarded osmosis (PRO) hollow fiber membranes with high power densities for renewable salinity-gradient energy generation, *Environ. Sci. Technol.*, 47 (2013) 8070–8077.
- [23] C.F. Wan, T.-S. Chung, Osmotic power generation by pressure retarded osmosis using seawater brine as the draw solution and wastewater retentate as the feed, *J. Membr. Sci.*, 479 (2015) 148–158.
- [24] X. Li, T.-S. Chung, Thin-film composite P84 co-polyimide hollow fiber membranes for osmotic power generation, *Appl. Energy*, 114 (2014) 600–610.
- [25] W. Gai, X. Li, J.Y. Xiong, C.F. Wan, T.-S. Chung, Evolution of micro-deformation in inner-selective thin film composite hollow fiber membranes and its implications for osmotic power generation, *J. Membr. Sci.*, 516 (2016) 104–112.
- [26] R.B. Carvalho, Hollow Fiber Composite Membranes for Nanofiltration and Reverse Osmosis Prepared by Immersion-Precipitation of Two Polymers Simultaneous Extrusion, PhD Thesis, Federal University of Rio de Janeiro, Brazil, 2005.
- [27] C.M. Hansen, Hansen Solubility Parameters, A User's Handbook, 2nd ed., CRC Press, Boca Raton, US, 2007.